Adsorption of 4-mercaptopyridine on Au(111): a periodic DFT study

Jan Kučera and Axel Groß
Institute for Theoretical Chemistry, Ulm University, D-89069 Ulm/Germany

We have studied the adsorption of 4-mercaptopyridine (Mpy) on Au(111) using periodic density functional theory calculations. Isolated Mpy molecules adsorb preferentially at near-bridge sites in a tilted configuration. The interaction with water influences the adsorption of Mpy only weakly whereas the binding of ions to Mpy can lead to substantial structural changes in the Mpy adsorption geometry. At higher coverages, the molecules become more upright in order to allow for a denser packing in the self-assembled monolayers (SAMs). Simulated STM images of the $7 \times \sqrt{3}$ and $5 \times \sqrt{3}$ structures compare favorably with experimental results. Using an ab initio thermodynamics approach, we determined the most stable molecular structure as a function of the chemical potential of mercaptopyridine. The stability of the $7 \times \sqrt{3}$ is confirmed, but the experimentally observed $5 \times \sqrt{3}$ structure does not appear as a thermodynamically stable structure. Several possible reasons for the discrepancy between theory and experiment are discussed.

I. INTRODUCTION

There is a strong current interest in the self-assembly of organic molecules on substrates as a path towards the design of nano-devices (see, e.g., Refs. [1–3]). Recently it has been demonstrated that thin metal films can be deposited on a self-assembled monolayer (SAM) of small aromatic thiols on gold [4–7]. These metal-molecule-metal structures can serve as a model system to study the transport through molecular electronic devices in order to understand metal-molecule interfacial phenomena in man-tailored nanoelectronics [8–10], but such a setup can also be used as a molecular sensing device [11, 12]. For the operation of such devices, the detailed knowledge of the microscopic geometrical arrangement at the metal-molecule interface is rather beneficial. However, in spite of numerous experimental and theoretical studies on the structure of the Au-S bond in SAMS made of thiolates, in particular methylthiolate [13–17], the exact nature of the molecule-metal interface is still debated. Diffraction and STM experiments together with electronic structure calculations indicate that the thiolate adsorption on Au(111) could induce a surface reconstruction involving defects such as Au adatoms [15–17], but also thiolate adsorption on bridge sites of flat terraces of Au(111) has been found [14, 17], as proposed by calculations [18, 19].

As a first step towards the characterization of the metal-molecule-metal structure we have studied the formation of self-assembled monolayers (SAMs) of 4-mercaptopyridine (Mpy) on Au(111) using periodic density functional theory (DFT) calculations. These molecules which consist of an aromatic ring with two functional groups opposite of each other have been used in the fabrication of the metal-molecule-metal contacts [4–9]. They are bound via the sulfur head group to the Au(111) substrate.

The structure of SAMs formed by Mpy on Au(111) has already been addressed in various scanning tunneling microscopy (STM) studies [20–23]. These STM experiments revealed that several different Mpy structures can exist on Au(111). Depending on the ambient conditions (solvent, concentration, pH, and applied potential), various densely-packed phases were observed and their structures identified as: (i) a long-striped superstructure with a rectangular $5 \times \sqrt{3}$ unit cell containing two Mpy molecules with a supposedly small S-S spacing [20, 21], a related $10 \times \sqrt{3}$ superstructure with four Mpy molecules per unit cell [22], (iii) a long striped superstructure with a $7 \times \sqrt{3}$ unit cell containing three separately binding Mpy molecules [23], and (iv) a dense superstructure supposedly within a $1 \times \sqrt{3}$ periodicity with only one Mpy molecule per unit cell [22, 23]. It should be noted that an exact structure determination in the STM experiments is not easy due to problems associated with the internal calibration using the known interatomic distances of the underlying substrate [22].

Whereas we are not aware of any first-principles electronic structure calculations addressing the interaction of Mpy with gold substrates, there are several DFT studies of thioorganic SAMs on gold using either cluster [24–26] or periodic slab models [27, 28] to describe the gold substrate. The adsorption structure of benzenethiol, a fundamental thioaromatic, on Au(111) was theoretically addressed based on periodic DFT calculations by Nara *et al* [29, 30]. They found that benzenethiolate molecules at low coverage are preferentially adsorbed on Au(111) with the S-head group at a bridge site slightly shifted toward the fcc-hollow site; the plane of the benzene ring is tilted by about $\sim 60°$ from the surface normal. The same minimum energy site was also identified for benzene-1,4-dithiol adsorption on gold in DFT cluster calculations [31, 32]. On the other hand, for a SAM formed by 4'-methyl-4-mercaptobiphenyl in the high-density regime within a $p(2\sqrt{3} \times \sqrt{2})R30°$ structure, the fcc-hollow adsorption site was found to be energetically most stable in DFT slab calculations [33].

We have studied the adsorption of Mpy on Au(111) both at low coverages and at high coverages using periodic DFT calculations. These calculations are performed for the substrate-vacuum interface. However, the thioaromatic SAMs are usually prepared in a solution of the appropriate organic thiol, and the STM studies

mentioned above were also carried out *in situ* in a liquid environment. Thus it is very likely that the adsorbed Mpy molecules are interacting with solvent molecules, leading for example to protonated Mpy. Unfortunately, the theoretical description of adsorbate structures at the solid-liquid interface is rather cumbersome [34–36]. As a preliminary step towards a more realistic treatment of the Mpy/Au interaction at the solid-liquid interface, we have also studied the interaction of an isolated Mpy-water complex and the protonated $MpyH^+$ form with Au(111). For the higher coverages, we have used an *ab initio* thermodynamics approach [37] in order to determine the thermodynamically stable Mpy structures on Au(111) as a function of the chemical potential of Mpy. Furthermore, we have simulated STM images in order to allow for a direct comparison with the experiment.

II. COMPUTATIONAL DETAILS

All calculations were performed using a periodic DFT package, the VASP code [38], using the generalized gradient approximation (GGA) to describe the exchange-correlation effects by employing the exchange-correlation functional by Perdew, Burke and Ernzerhof (PBE) [39]. The ionic cores were represented by projector augmented wave (PAW) potentials [40] as constructed by Kresse and Joubert [41]. The electronic one-particle wave function were expanded in a plane-wave basis set up to an energy cutoff of 400 eV.

The (111) surface of the Au electrode was modeled in the supercell approach by slabs with a thickness of three, five, or seven Au layers slabs and vacuum regions of 22, 19, and 15 Å thickness, respectively. The Au lattice spacing was adopted from the equilibrium geometry of bulk Au calculated at the same level of the theory. Within the particular model either one, two, or three topmost layers of gold were relaxed during the geometry optimization while the rest of the gold atoms was kept fixed at the positions corresponding to the bulk Au crystal.

Mercaptopyridine molecules adsorb as a thiolate, i.e. without the hydrogen atom of the S-H group. Therefore we refer the adsorption energy of Mpy on Au(111) to the free thiolate according to

$$E_{\mathrm{ads}} = E(\mathrm{C_5H_4NS/Au(111)} - [E(\mathrm{C_5H_4NS}) + E(\mathrm{Au(111)})] \,, \quad (1)$$

where $E(\mathrm{C_5H_4NS/Au(111)})$, $E(\mathrm{C_5H_4NS})$, and $E(\mathrm{Au(111)})$ are the total energies of Mpy adsorbed on Au(111), the Mpy(C_5H_4NS) radical in the gas phase, and the bare Au(111) surface, respectively. According to Eq. 1, exothermic adsorption is associated with a negative adsorption energy. In the following, we will refer to the *absolute* value of the adsorption energy as the binding energy. Note that in this energy balance the solvation energy of Mpy in the solution does not enter. However, taking this into account would only lead to a constant shift of all adsorption energies reported in this study but would not change the energetic ordering of the different structures.

To model the adsorption of single mercaptopyridine molecules (Mpy) on Au(111), a 3×3 surface unit cell was used corresponding to a coverage of 1 Mpy molecule per 9 Au atoms of the first surface layer. We will refer to this configuration as isolated Mpy molecules on Au(111) in the following. The Brillouin zone for such model was sampled with a uniform mesh of 25 k-points.

The calculated adsorption energies of Mpy on Au(111) change by less than 10 meV when the layer thickness is increased from three to five layers. Interestingly enough, the Mpy binding energies further increase by about 100 meV if the slab thickness is increased to seven layers. This fluctuation can be understood considering the fact that a metal slab corresponds to a quantum well system [42] which can lead to quantum confinement effects in calculated properties as a function of the slab thickness [43]. However, the energetic ordering of the Mpy/Au complexes (all optimized within the particular model) in the considered top fcc, fcc hollow, and bridge hollow sites (the structure explanation is described in the Result section) is not modified for thicker slabs. Because of the high computational cost associated with seven layer calculations and the sufficient accuracy of the three-layer calculations, all reported adsorption energies correspond to three-layer results with the uppermost layer allowed to relax, if not specified otherwise.

All structures were relaxed until the energy changed by less than 1×10^{-5} eV and until the residual forces are found to be less than 0.01 eV/Å. For several structures, we used an even more restrictive break condition by stopping the relaxation only when all forces were below 0.001 eV/Å. However, no different energy minimum structured resulted from this more accurate procedure. Although it is well-known that thiolate adsorption on Au(111) can induce surface reconstructions, as mentioned above [15–17], we only considered the flat Au(111) surface in our study because the computationally expensive investigation of surface reconstructions is beyond the scope of our systematic study focusing on the adsorption of Mpy on flat Au(111) alone.

III. RESULTS

A. Adsorption of isolated Mpy molecules on Au(111)

In order to determine the most stable adsorption sites of isolated Mpy molecules on Au(111), we have performed structure optimizations with different starting geometries involving various tilt angles between the S-C bond of the Mpy molecule and the Au(111) surface normal (denoted by $\theta_{\mathrm{Au-S-C}}$) as well as various azimuthal angles (denoted by ϕ; $\phi = 0^\circ$ corresponds to the [110] direction along one of the axes of the 3×3 surface cell of Au(111).

We found six stable and metastable adsorption sites of

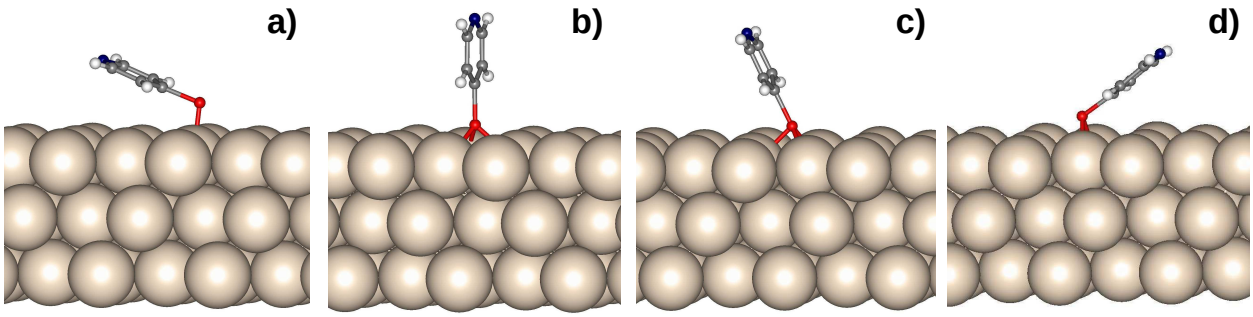

FIG. 1: Optimized structure of an isolated mercaptopyridine molecule adsorbed on Au(111) within a 3×3 periodicity at a) the top-fcc, b) fcc upright ($\theta_{\mathrm{Au-S-C}}$=0.0 °), c) fcc tilted ($\theta_{\mathrm{Au-S-C}}$=26 °) , and d) bridge-fcc site, respectively.

Mpy on Au(111): top-fcc, top-hcp, fcc hollow, hcp hollow, bridge-fcc, and bridge-hcp, that are abbreviated as t-fcc, t-hcp, fcc, hcp, b-fcc, and b-hcp, respectively, in the following. This nomenclature which has been used before [29, 30] means that for example in the b-fcc configuration the S atom is located at a bridge site slightly shifted toward the fcc-hollow site. In addition, new labels t-fcc and t-hcp are introduced in order to distinguish two top sites in which the S-head group is slightly shifted toward the fcc and hcp hollow site, respectively. Table I lists the adsorption energies and the geometry parameters of all the six structures. The adsorption geometries at the t-fcc, fcc and b-fcc site are illustrated in Fig. 1. The Mpy/Au complexes are stabilized *via* the strong interaction between the Mpy sulfur head group and either one-, two-, or three gold atoms of the first Au layer at the top, bridge and hollow sites, respectively.

In the energy minimum configurations, the S-C bond is significantly tilted from the surface normal (the corresponding angle θ_{Au-S-C} ranges from 26 to 70°). The only exception is the fcc site where the up-right geometry (θ_{Au-S-C}=0°) and the tilted geometry are energetically degenerate within the accuracy of our calculations. In the most stable sites, the azimuthal angle ϕ corresponds is either 0° or 180° (note that due to the tilting of Mpy, $\phi = 0°$ and $\phi = 180°$ are in general not equivalent).

The strongest binding of Mpy to Au(111) is found at the bridge site with adsorption energies of -1.415 and -1.400 eV in the b-fcc and b-hcp configurations, respectively. As Table I demonstrates, the adsorption structures of Mpy at the b-fcc (Fig. 1c) and b-hcp sites are very similar. For both sites, the distance to the two nearest Au atoms forming the bridge is 2.51 Å whereas the distances between S and the third nearest Au atom are 3.18 and 3.22 Å in the b-fcc and b-hcp configuration, respectively. The tilting angles θ_{Au-S-C} are also almost the same in both configurations. At the bridge site the S-C bond is slightly tilted from the plane of the Mpy aromatic ring, yielding a dihedral angle of ∼5°.

All other adsorption sites are energetically less favorable by 0.185, 0.257, 0.235, and 0.243 eV at the fcc, hcp, t-fcc, and t-hcp site, respectively. At the hollow sites the binding is three-fold coordinated. Due to the high coordination of the sulfur atom at this site, the Mpy molecule shows the most upright orientation of all sites. In fact, there are two stable states, one upright configuration (Fig. 1b) and one slightly tilted one (Fig. 1c) which is less stable by 14 meV and also exhibits slightly longer S-Au bonds (see Table I). Note that within the accuracy of the DFT calculations these two configurations have to be considered as being energetically degenerate. Indeed, in calculations using a five-layer Au slab, the energetic difference between the two configurations practically vanishes (∼ 1 meV). The adsorption complex at the hcp hollow site, on the other hand, is considerably less stable than those at the fcc hollow site. This difference is also reflected by the fact that the S-Au bond of the Mpy/Au complex at the fcc site is shorter by about ∼ 0.09-0.16Å than at the hcp site. In addition, at the hcp site the tilted configuration of Mpy is more preferable than the up-right configuration.

At the top site, where the Mpy is only bound to one

TABLE I: Adsorption energies and geometry parameters of the Mpy molecule adsorbed at the top-fcc, top-hcp, hcp hollow, fcc hollow, bridge-hcp, and bridge-fcc sites of Au(111). The relaxation energy E_{rel} corresponds to the change in the adsorption energy when the first Au layer is allow to relax in the calculations instead of being fixed. $d_{\mathrm{S-Au}}$ corresponds to the distance of the sulfur atom to the nearest Au atoms where $\theta_{\mathrm{Au-S-C}}$ is the angle between the S-C bond of the Mpy molecule and the Au(111) surface normal.

Site	E_{ads} (eV)	E_{rel}(eV)	$d_{\mathrm{S-Au}}$ (Å)	$\theta_{\mathrm{Au-S-C}}$ (°)
t-fcc	-1.180	-0.029	2.41	68
t-hcp	-1.172	-0.030	2.40	65
fcc tilted	-1.216	-0.144	2.57 2.57 2.49	26
fcc upright	-1.230	-0.221	2.49 2.49 2.52	0
hcp	-1.158	-0.072	2.64 2.64 2.61	43
b-fcc	-1.415	-0.097	2.51 2.51 *3.18*	55
b-hcp	-1.400	-0.092	2.51 2.51 *3.22*	52

Au atom, the Mpy molecule shows the strongest tilt with respect to the surface normal (Fig. 1a) with the aromatic ring being almost parallel to the surface. Because of the one-fold coordination, the S-Au distance is the smallest of all adsorption sites with only small differences between the t-fcc and t-hcp configuration. The S-C bond is slightly tilted from the plane of the Mpy aromatic ring by about $\sim 3°$.

The relaxation of the surface plays a relatively strong role for the adsorption. The relaxation energy E_{rel} listed in Table I corresponds to the change in the adsorption energy when the first Au layer is allowed to relax instead of being fixed. This relaxation energy is correlated with the coordination (except for the hcp site) being strongest for the fcc site where it amounts to -0.143 eV and -0.221 eV for the two stable configurations. At the top sites, the influence of the substrate relaxation is the weakest leading to a gain in the binding energies of less than 30 meV. Note that the inclusion of the surface relaxation leads to a reversal in the energetic preference between the top site and the fcc site and also between the fcc and the hcp site.

Our findings with respect to the adsorption energies and geometries of Mpy on Au(111) are very similar to those for the adsorption of benzenethiol [29, 30, 44] where only the N atom is replaced by a CH group. This indicates that the Au-S bond is only weakly influenced by modifications of the aromatic system.

Furthermore, the preference for the bridge site slightly shifted toward the hollow site is also found for other thioaromatics such as benzene-1,4-dithiol [31, 32]. This site preference has been explained by the lower steric repulsion at these sites between the gold surface and the sulfur back bond [45]. However, in contrast to the studies on benzenthiol [29, 30] we found that also an upright Mpy geometry is stable at the fcc site.

B. Diffusion barriers of Mpy on Au(111)

Depending on the ambient conditions (solvent, concentration, pH, and applied potential), different Mpy structures were found on Au(111) [20–23]. In this context, the Mpy diffusion barriers are of interest in order to see how easily these structures can be formed and transformed. To estimate the energy barriers between the particular sites on the Au surface, potential energy curves were determined as a function of the Mpy displacement along the $[\bar{2}11]$ direction of the (111) surface passing through the bridge, three-fold hollow and top sites (see inset Fig. 2).

Two different azimuthal orientations denoted by *OI* and *OII* were considered with azimuthal angles $\phi = 0°$ and $\phi = 180°$ corresponding to molecules with tilt angles in opposite directions. The Mpy molecule was moved in such way that the S-head was translated and then the whole molecule was relaxed except for the lateral coordinates of the sulfur atom so that also the tilt angle could change. The fact that the potential curves for the two azimuthal orientations shown in Fig. 2 differ in general

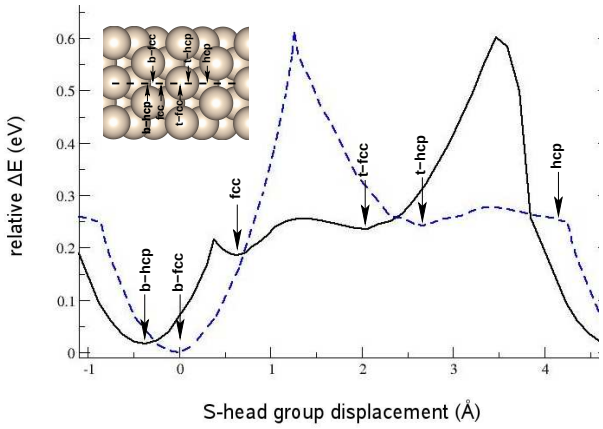

FIG. 2: Potential energy curve calculated as a function of displacement of Mpy in orientation *OI* (solid line) and *OII* (dashed line) along the path from b-hcp to hcp site going through b-fcc, fcc, t-fcc, and t-hcp sites on Au(111) surface. The path and the corresponding sites are illustrated in the inset.

demonstrates that these two oppositely tilted configurations are locally stable on the Au(111) surface.

The potential curve for the *OI* orientation passes through the main minimum and two local minima corresponding to Mpy at the b-hcp, t-fcc, and fcc sites, respectively whereas the potential energy path *OII* goes through the main minimum at the b-fcc sites and two local minima at the hcp and t-hcp sites. Note that there are no local minima corresponding to the hcp site for the *OI* orientation and to the fcc site for the *OII* orientations. The results indicate that the potential energy surface is rather flat between the hollow and the top site. To reach this plateau from the most favorable adsorption sites requires only about 0.2 eV, with additional barriers of ~ 0.37 eV to propagate from the t-fcc to the b-hcp site and of ~ 0.36 eV from the t-hcp to the b-fcc site with fixed azimuthal orientation.

According to Fig. 2, the two different configurations of the Mpy molecule at the b-hcp and b-fcc sites seem to be separated by a relatively small barrier. However, it is important to note that the two curves in Fig. 2 correspond to the two orientations *OI* and *OII*, and the propagation from the *OII* orientation at the b-fcc site to the *OI* orientation at the b-hcp site requires also a flipping of the orientation. In order to find the lowest diffusion path between these configurations, we employed the nudged elastic band method [46] which is an automatic transition state search routine. Flipping the Mpy molecule from one orientation to the other at a specific site, say, the b-hcp site, requires to overcome a barrier of 0.36 eV. Interestingly enough, using seven so-called images for the determination of the propagation path [46] we found that it is energetically less costly if the molecule first moves from the b-fcc site to the fcc site, changes its orienta-

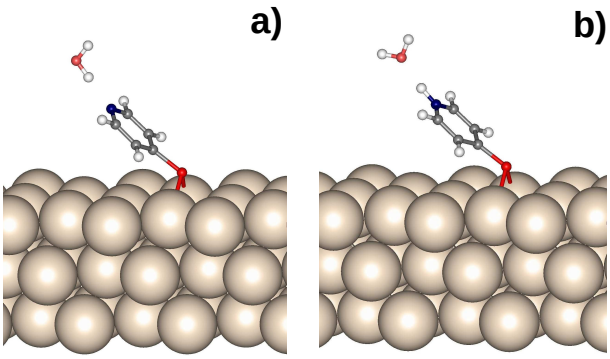

FIG. 3: Calculated energy minimum structures of $H_2O\cdots$Mpy (a) and $H_2O\cdots MpyH^+$ (b) adsorbed at the energetically most favorable b-fcc site on Au(111).

tion there with the transition state corresponding to the upright configuration, and then propagates back in the other orientation towards the b-hcp site. This path is only hindered by a barrier of 0.19 eV. Irrespective of the details of the diffusion path, these results show that in general the diffusion barriers are rather low allowing a facile restructuring of the Mpy molecules on Au(111).

C. Adsorption of $H_2O\cdots$Mpy, $MpyH^+$, and $H_2O\cdots MpyH^+$ on Au(111)

The experiments studying the formation of Mpy-SAMs were all performed in solution whereas no electrolyte was considered in our calculations so far. In order to get an idea about the influence of the electrolyte on the adsorption of Mpy on Au(111), we calculated the adsorption properties of Mpy at the b-fcc and fcc sites with H^+, H_2O and H_2O-H^+ attached to the nitrogen atom in the low coverage regime using a 3×3 surface unit cell. The protonated systems were described by removing one electron per supercell which was compensated by an uniform background charge distribution in order to avoid the divergence of the electrostatic energy. The resulting structural and energetic parameters for these adsorption complexes are summarized in Table II.

The minimum energy structure of the $H_2O\cdots$Mpy complex at the b-fcc site of Au(111) is shown in Fig. 3a. The water molecule interacts with the Mpy molecule on Au(111) *via* a hydrogen bond (H-bond) to the nitrogen atom of Mpy. The interaction or adsorption energies of the water molecule defined as $E_{int} = E$ ($H_2O\cdots$Mpy/Au) - [E(Mpy/Au) + E(H_2O)], are -0.278 and -0.293 eV for the b-fcc and fcc complex, respectively, which corresponds in fact to typical adsorption energies of water monomers at electrode surfaces [35, 47]. The interaction of water with the Mpy hardly changes the distances d_{S-Au} between the sulfur atom and the nearest Au atoms (compare with Table I) which indicates that the formation of the weak $H_2O\cdots$Mpy complex does not influence the strength of the S-Au bonding. Consequently, also the energetic ordering between the b-fcc and fcc adsorption sites remains almost identical to the case without water.

In contrast, the S-Au distances are enlarged by about ∼0.1 and 0.14-0.2 Å for the b-fcc and fcc site, respectively, when Mpy becomes protonated. Furthermore, the absolute value of the relaxation energy ΔE_{rel} decreases by 0.10 and 0.03 eV for the tilted configurations at the fcc and b-fcc sites, respectively, compared to the corresponding values of ΔE_{rel} for the non-protonated cases given in Table I. Although the angle θ_{Au-S-C} changes only by $\sim 4°$ at the b-fcc site, these findings imply that the protonization causes a weakening of the Mpy-Au interaction which also lowers the energetic preference for the b-fcc adsorption site. In addition, the protonation makes the interaction of water with Mpy stronger. The water molecule is bound with its oxygen molecule to the $MpyH^+$/Au complex (see Fig. 3b), and the interaction energy is −0.658 eV at both adsorption sites. In spite of this stronger bonding, the S-Au interaction of $MpyH^+$ is again hardly changed by the presence of water indicated by the small changes in the S-Au distances upon water adsorption, as Table II demonstrates.

We admit that our modeling of solvent effects in the adsorption of Mpy is rather approximate. Furthermore, it should be mentioned that the introduction of a compensating charge background throughout the unit cell creates spurious interactions with the electrons that might lead to artefacts in the results [48]. However, these artefacts should not influence the qualitative conclusions of this section, namely that the interaction with water influences the adsorption structure of Mpy only weakly, whereas the adsorption of ions on Mpy can well lead to structural changes of the molecules. We have performed additional preliminary calculations in which we included a whole water layer on top of the dense Mpy structures on Au(111) discussed in the next section. These calculations show that the effect of a pure water layer on the adsorbates is very weak, as also found in other studies [35, 36], which is consistent with the conclusions based on the one-water molecule model.

D. Higher coverages of Mpy on Au(111)

Finally, we address the structure of Mpy at higher coverages as found in the experiment. We considered $7\times\sqrt{3}$ and $5\times\sqrt{3}$ Mpy structures on Au(111) which were identified in STM experiments under various electrochemical conditions [20, 23]. In addition, we studied Mpy adsorption within a $\sqrt{3}\times\sqrt{3}$ surface unit cell which is typically found for SAMs made from alkanethiolates [27]. Such a structure has to the best of our knowledge not been observed for Mpy on Au(111) yet, but it has been found for other aromatic thiols adsorbed on Au(111) [49]. The

TABLE II: Adsorption of $H_2O\cdots$Mpy, $MpyH^+$, and $H_2O\cdots MpyH^+$ on Au(111) in a 3×3 surface unit cell: relative stability ΔE_{tot} of the tilted configuration at the fcc site with respect to the b-fcc site, distances d_{S-Au} between the sulfur atom of Mpy and the nearest Au atoms, and change of the relaxation energy ΔE_{rel} with respect to the adsorption of pure Mpy (see Table I).

System	Site type	ΔE_{tot} (eV)	d_{S-Au} (Å)	ΔE_{rel} (eV)
$H_2O\cdots$Mpy/Au	fcc	0.187	2.58 2.58 2.50	-0.124
	b-fcc	0.0	2.50 2.50 3.14	-0.080
$MpyH^+$/Au	fcc	0.139	2.81 2.81 2.63	-0.047
	b-fcc	0.0	2.61 2.61 3.29	-0.067
H_2O/$MpyH^+$/Au	fcc	0.139	2.79 2.79 2.60	-0.049
	b-fcc	0.0	2.59 2.59 3.26	-0.070

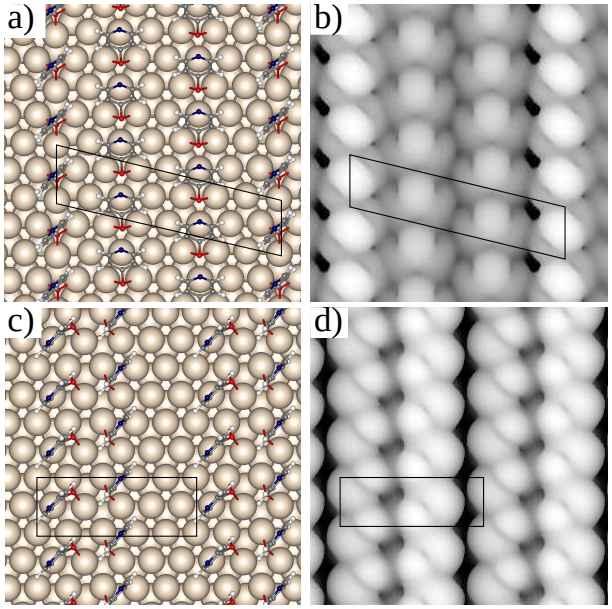

FIG. 4: Optimized configuration together with a simulated STM image for Mpy/Au in the $7 \times \sqrt{3}$ (a,b) and the $5 \times \sqrt{3}$ structure (c,d).

Mpy coverages per Au atom in these structures correspond to 3/14, 1/5 and 1/3 for the $7 \times \sqrt{3}$, $5 \times \sqrt{3}$, and $\sqrt{3} \times \sqrt{3}$ structures, respectively.

From the STM measurements, the periodicity of a specific SAM can be derived, however, the microscopic structure within the unit cell can not be determined unambiguously. In particular, there is no direct information on the precise adsorption sites of the molecules within the unit cell. Therefore we performed a careful structural search for the energy minimum configurations. The structural analysis was carried out by a relaxation from various initial structures. The set comprised all stable geometries found for Mpy at low coverage. Furthermore, we considered also up-right structures in addition to the tilted geometries for all sites. In the case of the $7 \times \sqrt{3}$ periodicity we started from the assumption [8] that the two Mpy molecules forming two parallel stripes in $[1\bar{1}0]$ direction occupy equivalent sites while the third molecule is turned by 60°. We first searched for the most stable structure of only one Mpy molecule (Mpy1) per unit cell. After that we included the other two molecules Mpy2 and Mpy3 in the calculations. Keeping Mpy1 and Mpy 2 parallel in equivalent sites and Mpy3 turned by 60° we finally probed various arrangements of all three molecules. The resulting optimal structures for the $7 \times \sqrt{3}$ and $5 \times \sqrt{3}$ geometries are illustrated in Fig. 4. In addition, we simulated STM images using the Tersoff-Hamann approach [50] in order to allow for a direct comparison with the experiment. The corresponding structural parameters are collected in Tab. III.

As far as the $7 \times \sqrt{3}$ structure is concerned, there are 3 inequivalent Mpy molecules per surface unit cell in the most stable structure. Two Mpy molecules, denoted by Mpy1 and Mpy2, are located at b-fcc sites within an almost identical arrangement whereas the third molecule Mpy3 is located at the hollow site (see Fig. 4a). The average value of the adsorption energy E_{ads} per molecule is −1.376 eV which is slightly more stable than the average value of −1.353 eV associated with two isolated Mpy molecules at the b-fcc site and one isolated Mpy

TABLE III: High-coverage structures of Mpy on Au(111). Adsorption energies E_{ads} per Mpy molecule and structural parameters as defined in Tab. I for the individual Mpy molecules in the energetically most stable configurations found for the $7 \times \sqrt{3}$, $5 \times \sqrt{3}$, and $\sqrt{3} \times \sqrt{3}$ structures on Au(111). Note that adsorption energy E_{ads} corresponds to the average value per unit cell.

Symmetry	E_{ads} (eV)	molecule	site	d_{S-Au} (Å)	θ_{Au-S-C} (°)
$7 \times \sqrt{3}$	-1.376	Mpy1	b-fcc	2.49 2.52 *3.12*	47
		Mpy2	b-fcc	2.49 2.50 *3.13*	48
		Mpy3	fcc	2.54 2.55 2.57	9
$5 \times \sqrt{3}$	-1.315	Mpy1	b-fcc	2.42 2.53 *3.09*	37
		Mpy2	b-hcp	2.42 2.63 *2.94*	48
$\sqrt{3}\times\sqrt{3}$	-1.104	Mpy1	b-fcc	2.49 2.49 3.08	34

molecule at the fcc hollow site (see Table I). Although the difference is rather small, this still indicates that there should be some attractive interaction between the Mpy molecules.

The lengths of the S-Au bonds of the Mpy1 and Mpy2 molecules at the b-fcc sites are very similar to those of the isolated adsorbed Mpy molecule; the planes of their aromatic ring are practically parallel to each other and they are still tilted significantly with respect to the surface normal but less than the isolated Mpy molecule at the b-fcc site because of the mutual interaction. The Mpy3 molecule, on the other hand, stands almost upright and its aromatic ring is rotated by about ∼30° with respect to the densely packed rows of the (111) surface.

In the $5 \times \sqrt{3}$ structure, there are two Mpy molecules per surface unit cell. Based on STM measurements, the existence of a dithiopyridine species in this structure was proposed [20, 21]. We placed dithiopyridine on several sites of the $5 \times \sqrt{3}$ unit cell, but could not find any stable adsorption complex with the sulfur headgroups forming a S-S dimer. Hence we have to rule out the existence of dithiopyridine on flat Au(111) based on our DFT calculations. As the most stable arrangement with the sulfur atoms about one Au lattice unit apart we find the configuration shown in Fig. 4c where the shortest S-S distance is 3.1 Å. The adsorption energy per Mpy molecule is $E_{ads} = -1.315\,\text{eV}$, which means that the binding is slightly weaker in the $5 \times \sqrt{3}$ structure than in the $7 \times \sqrt{3}$ structure, in spite of the lower density. The sulfur head groups of both Mpy molecules are located at bridge sites. In contrast to the low-density case, the planes of the aromatic rings of the Mpy molecules are now oriented upright with respect to the surface, however, the S-C bond of the two Mpy molecules are tilted 37° and 48° away from the surface normal in opposite directions.

The simulated STM images for the $7 \times \sqrt{3}$ and structure $5 \times \sqrt{3}$ structure also shown in Fig. 4 compare well with the corresponding experimental in-situ high resolution STM images [20, 23], giving additional creditability to our structure determination. Note that the elongated bright structures in Figs. 4 b and d do not correspond to the plane of the aromatic ring; they are rather oriented perpendicular to the aromatic ring. An analysis of the local density of states suggests that this feature is mainly related to the lone pair at the nitrogen atom which is relatively weakly coupled to the π electron system of the Mpy molecule [51].

Figure 5 shows the optimized configuration of Mpy/Au(111) within a hypothetical $\sqrt{3} \times \sqrt{3}$ structure where there is only one Mpy molecule per unit cell. Again, we identify the bridge site as the energetically most stable site, however, within this periodicity it is only about 0.035 eV more stable per molecule than the corresponding structure with all Mpy molecules at the hollow site. When we considered 5 Au layers in the calculations, the difference increased to 0.065 eV which is still less pronounced than for the corresponding sites at low coverages. The Mpy molecules at the hollow sites have

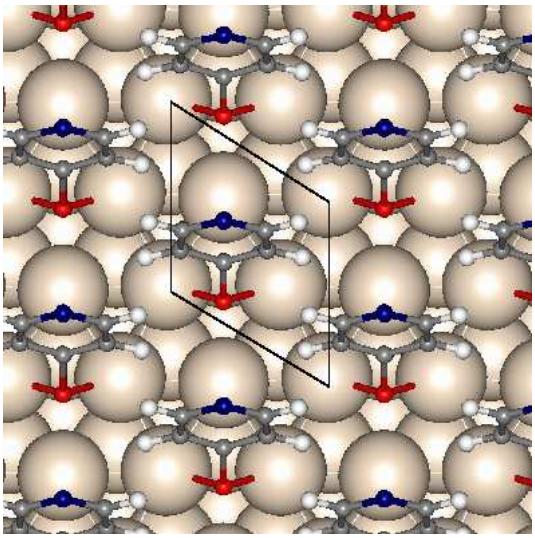

FIG. 5: Optimized configuration for Mpy within the $\sqrt{3}\times\sqrt{3}$ periodicity on Au(111).

an upright geometry, whereas the Mpy molecules sitting at the b-fcc sites are still tilted, however, the S-C bond is more upright by about 21° compared to the isolated adsorbed Mpy molecule. Furthermore, the plane of the aromatic ring is more tilted away from the S-C bond by about 7° compared to the isolated Mpy molecules at the bridge site. Calculations for Mpy molecules within this tilted configuration in the gas-phase demonstrate that it is the energetic cost of this deformation that reduces the energy difference between the bridge and hollow sites in the dense structures.

Summarizing the results for the considered Mpy structures at higher coverages, we note that the bridge site remains the energetically most preferential site. The three-fold hollow sites will become occupied when the bridge sites are blocked due to, e.g., steric hindrance. The top sites are not occupied at higher coverage although top and three-fold hollow sites are energetically almost degenerate at low coverage. This is due to the fact that the higher coverage requires a more upright configuration which is energetically more costly at the top site which exhibits the largest tilt angle with respect to the surface normal at low coverage.

As far as higher coverages of Mpy on Au(111) are concerned, there is an attractive interaction between the π systems of the molecules due to dispersive forces. However, dispersion is not correctly reproduced within the DFT approach using GGA functionals. In order to estimate the strength of this attractive π-π interaction, we performed MP2 calculations for two isolated parallel Mpy molecules as a function of their distance, using an atomic centered aug-cc-pVDZ basis set. In these calculations, we found a maximum attractive interaction of $\sim 0.2\,\text{eV}$ (counterpoise corrected) at a distance of 3.7 Å. This intermolecular distance is very similar to the equilibrium

distance of 3.8 Å found for the benzene dimer in the parallel configuration at the same level of theory [52] yielding a stabilization energy 0.12 eV. Yet, it is well-known that MP2 significantly overbinds dispersion complexes. Consequently, at the CCSD(T)/aug-cc-pVQZ level the stabilization energy between the two benzene molecules is reduced to 0.07 eV at a distance of 3.9 Å.

It should furthermore be noted that the distances between the Mpy molecules in the considered high-coverage structures are about ~ 5 Å. On the other hand, the Mpy molecules in the high-coverage structures are still tilted thus reducing the distance between the planes of the aromatic rings. Therefore it is certainly desirable to accurately determine the contribution of dispersion to the interaction between the Mpy molecules, in particular with respect to the small differences in the adsorption energy between the considered structures.

E. Thermodynamically stable structures of Mpy on Au(111)

We have calculated the adsorption Mpy energies for different structures and coverages. In fact, we find the strongest adsorption for the isolated molecules within the 3×3 arrangement indicating steric hindrance between the adsorbed Mpy molecules at higher coverages. Still, dense Mpy structures have been found in experiments. In order to understand the stability of these structures, one has to take into account that upon the formation of the SAM the adsorbed Mpy molecules are in contact with a reservoir of Mpy molecules in solution. This reservoir can be characterized by its chemical potential μ which is a function of temperature, concentration, etc. To determine the stable adsorption structure in thermal equilibrium with a reservoir, a thermodynamical concept recently applied to study the stability of surface oxides in heterogeneous catalysis at non-zero temperatures and pressures from first principles [37] can be used. This concept was already applied to the adsorption of acrolein on Pt(111) as a function of temperature and pressure [53]. It is based on the Gibbs free energy of adsorption $\Delta\gamma$ [37] which at the solid-liquid interface is a function of the temperature T and the concentration c,

$$\begin{aligned}\Delta\gamma(T,c) &= \gamma(T,c,N_{\rm ads}) - \gamma_{\rm clean}(T,c,0) &(2)\\ &= \frac{1}{A}\Delta G^{ads}(T,c) &(3)\\ &= \frac{N_{\rm ads}}{A}\left(E_{\rm ads} - \mu_{\rm ads}(T,c)\right)\ , &(4)\end{aligned}$$

where $N_{\rm ads}$ is the number of adsorbed molecules per surface unit cell area A, $\mu_{\rm ads}(T,c)$ is the chemical potential of the adsorbate, and $E_{\rm ads}$ is the adsorption energy which can for example be derived from *ab initio* total-energy calculations using Eq. (1). In the derivation of Eq. (4), entropic contributions to the free energy have been neglected since they are typically rather small [37].

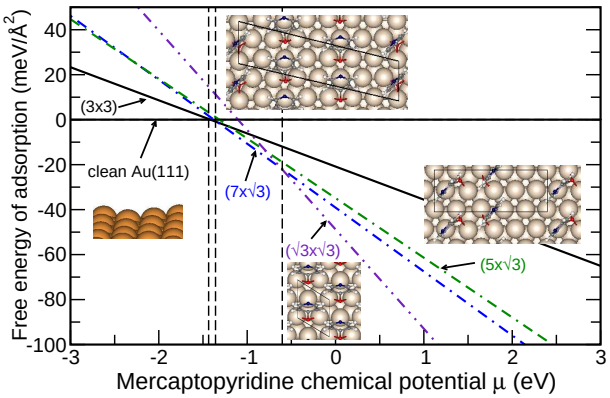

FIG. 6: Free surface energies of 4-mercaptopyridine on Au(111) as a function of the chemical potential. The vertical dashed lines indicate the stability range of the different considered structures which are illustrated in the insets. The $(5\times\sqrt{3})$ structure (green dashed line) is not stable for any given value of μ according to the DFT calculations.

The free energy of adsorption $\Delta\gamma$ yields the stable adsorbate structure as a function of the chemical potential which itself is a function of temperature, concentration, etc. For ideal solutions, the chemical potential is given by

$$\mu(T,c) = \bar{\mu}(T,c_0) + k_{\rm B}T\ln\left(\frac{c}{c_0}\right)\ , \qquad (5)$$

where $\bar{\mu}$ is the chemical potential at standard conditions. Deviations from the standard behavior are usually accounted for by replacing the concentration by the activity $a = f\cdot c$ where f is the activity coefficient that can for example be calculated using the Debye-Hückel equation [54]. However, we made no attempt to determine such a quantitative relation since we are only interested in the order of stability as a function of increasing chemical potential which is monotonically related to the concentration.

In Fig. 6, $\Delta\gamma$ is plotted for several mercaptopyridine structures on Au(111). The adsorption energy $E_{\rm ads}$ entering (4) was calculated for the mercaptopyridine radical according to Eq. (1). For a given chemical potential, the adsorbate structure with the lowest free energy is the stable one in thermal equilibrium. Note that within this formalism environment-dependent free energies of adsorption can be evaluated without taking the environment explicitly into account.

As Fig. 6 demonstrates, the experimentally observed $7\times\sqrt{3}$ structure [23] is indeed thermodynamically stable in a certain range of the mercaptopyridine chemical potential. However, according to Fig. 6 the likewise observed $5\times\sqrt{3}$ structure [22] should not be thermodynamically stable. Furthermore, for higher chemical potentials corresponding, e.g., to a higher concentration of mercaptopyridine a $\sqrt{3}\times\sqrt{3}$ structure should become stable that had not been identified in experiments yet.

There are several possible explanations for the discrepancies between theory and experiment. First of all, the energy differences between the various structures are rather small and are well within the accuracy of the DFT calculations. Actually, the fact that the free energies of adsorption of the $7 \times \sqrt{3}$ and the $5 \times \sqrt{3}$ structures are so similar means that subtle details of the preparation apparently determine the particular structure of the SAM that is eventually formed. This is in fact reflected in the electrochemical STM experiments which found that the observed pyridine structures depend sensitively on the choice of the electrolyte [23].

There are additional sources for errors in the calculations. As already mentioned, the DFT calculations do not reproduce the attractive van der Waals interaction between Mpy molecules which make the denser structures energetically more favorable. On the other hand, in the experiment the adsorbed mercaptopyridine thiolate might form complexes with anions from the solution. The electrostatic interaction between the charged complexes would lead to an additional repulsion between the adsorbed molecules and thus destabilize the high-density structures. One can also not rule out that the experimentally observed structures do not correspond to an equilibrium situation but are rather metastable. Further theoretical and experimental investigations are obviously needed, but the analysis of the free energy of SAMs is certainly indispensable for a true comparison between theory and experiment.

IV. CONCLUSIONS

The adsorption of 4-mercaptopyridine (Mpy) on Au(111) in different configurations and for various coverages has been studied by periodic density functional theory calculations. The near-bridge site, which is the energetically most stable site for isolated Mpy molecules, is also preferentially occupied in the denser, experimentally observed $7 \times \sqrt{3}$ and $5 \times \sqrt{3}$ structures. The microscopic site assignment for these self-assembled monolayers (SAMs) is substantiated by simulated STM images that compare favorably well with experimental images.

According to the calculated free energy of adsorption as a function of the chemical potential of Mpy, the $7 \times \sqrt{3}$ structure is indeed thermodynamically stable whereas the $5 \times \sqrt{3}$ structure does not correspond to a free energy minimum structure. On the other hand, the hypothetical $\sqrt{3} \times \sqrt{3}$ geometry should become stable at higher Mpy concentrations. The discrepancy between experiment and theory could be due to limitations of the DFT exchange-correlation functionals which for example do not reproduce the attractive van der Waals interaction between the molecules. Another severe approximation is the neglect of the solvent in the calculations since in particular the specific adsorption of ions can significantly influence the adsorption structure of the adsorbed Mpy molecules. These issues will be the topic of further studies.

Acknowledgments

Financial support by the Deutsche Forschungsgemeinschaft (DFG) within SFB 569 is gratefully acknowledged. We thank our colleagues H.-G. Boyen, T. Jacob, J. Keith, D.M. Kolb, B. Koslowski, Ch. Wöll, and P. Ziemann for useful discussions.

[1] Ulman, A. *Chem. Rev.* **1996**, *96*, 1533–1554.
[2] Love, J. C.; Estroff, L. A.; Kriebel, J. K.; Nuzzo, R. G.; Whitesides, G. M. *Chem. Rev.* **2005**, *105*, 1103–1169.
[3] Meier, C.; Landfester, K.; Künzel, D.; Markert, T.; Groß, A.; Ziener, U. *Angew. Chem. Int. Ed.* **2008**, *47*, 3821.
[4] Baunach, T.; Ivanova, V.; Kolb, D. M.; Boyen, H.-G.; Ziemann, P.; Büttner, M.; Oelhafen, P. *Adv. Mater.* **2004**, *16*, 2024.
[5] Ivanova, V.; Baunach, T.; Kolb, D. M. *Electrochim. Acta* **2005**, *50*, 4283.
[6] Manolova, M.; Ivanova, V.; Kolb, D. M.; Boyen, H.-G.; Ziemann, P.; Büttner, M.; Romanyuk, A.; Oelhafen, P. *Surf. Sci.* **2005**, *590*, 146.
[7] Manolova, M.; Kayser, M.; Kolb, D. M.; Boyen, H.-G.; Ziemann, P.; Mayer, D.; Wirth, A. *Electrochim. Acta* **2007**, *52*, 2740–2745.
[8] Boyen, H.-G.; Ziemann, P.; Wiedwald, U.; Ivanova, V.; Kolb, D. M.; Sakong, S.; Groß, A.; Romanyuk, A.; Büttner, M.; Oelhafen, P. *Nature Mater.* **2006**, *5*, 394.
[9] Shekhah, O.; Busse, C.; Bashir, A.; Turcu, F.; Yin, X.; Cyganik, P.; Birkner, A.; Schuhmann, W.; Wöll, C. *Phys. Chem. Chem. Phys.* **2006**, *8*, 3375–3378.
[10] Groß, A. *J. Comput. Theor. Nanosci.* **2008**, *5*, 894.
[11] Dong, X.; Xia, Y.; Zhu, G.; Zhang, B. *Nanotechnolgy* **2007**, *18*, 395502.
[12] Manolova, M.; Boyen, H.-G.; Kučera, J.; Groß, A.; Romanyuk, A.; Oelhafen4, P.; Ivanova, V.; Kolb, D. M. Adv. Mater., in press, **2008**.
[13] Kondoh, H.; Iwasaki, M.; Shimada, T.; Amemiya, K.; Yokoyama, T.; Ohta, T.; Shimomura, M.; Kono, S. *Phys. Rev. Lett.* **2003**, *90*, 066102.
[14] Maksymovych, P.; Sorescu, D. C.; John T. Yates, J. *J. Phys. Chem. B* **2006**, *110*, 21161.
[15] Maksymovych, P.; Sorescu, D. C.; John T. Yates, J. *Phys. Rev. Lett.* **2006**, *97*, 146103.
[16] Yu, M.; Bovet, N.; Satterley, C. J.; Bengio, S.; Lovelock, K. R. J.; Milligan, P. K.; Jones, R. G.; Woodruff, D. P.; Dhanak, V. *Phys. Rev. Lett.* **2006**, *97*, 166102.
[17] Mazzarello, R.; Cossaro, A.; Verdini, A.; Rousseau, R.; Casalis, L.; Danisman, M. F.; Floreano, L.; Scandolo, S.; Morgante, A.; Scoles, G. *Phys. Rev. Lett.* **2007**, *98*, 016102.

[18] Vargas, M.; Giannozzi, P.; Selloni, A.; Scoles, G. *J. Phys. Chem. B* **2001**, *105*, 9509.
[19] Hayashi, T.; Morikawa, Y.; Nozoye, H. *J. Chem. Phys.* **2001**, *114*, 7615.
[20] Sawaguchi, T.; Mizutani, F.; Taniguchi, I. *Langmuir* **1998**, *14*, 3565–3569.
[21] Wan, L.; Hara, Y.; Noda, H.; Osawa, M. *J. Phys. Chem. B* **1998**, *102*, 5943–5946.
[22] Baunach, T.; Ivanova, V.; Scherson, D. A.; Kolb, D. M. *Langmuir* **2004**, *20*, 2797.
[23] Zhou, W.; Baunach, T.; Ivanova, V.; Kolb, D. M. *Langmuir* **2004**, *20*, 4590.
[24] Akinaga, Y.; Nakajima, T.; Hirao, K. *J. Chem. Phys.* **2001**, *114*, 8555–8564.
[25] Sellers, H.; Ulman, A.; Shnidman, Y.; Eilers, J. E. *J. Am. Chem. Soc.* **1993**, *115*, 9389–9401.
[26] Beardmore, K. M.; Kress, J. D.; Grønbech-Jensen, N.; Bishop, A. R. *Chem. Phys. Lett.* **1998**, *286*, 40–45.
[27] Yourdshahyan, Y.; Zhang, H. K.; Rappe, A. M. *Phys. Rev. B* **2001**, *63*, 081405.
[28] Morikawa, Y.; Hayashi, T.; Liew, C. C.; Nozoye, H. *Surf. Sci.* **2002**, *507*, 46–50.
[29] Nara, J.; Higai, S.; Morikawa, Y.; Ohno, T. *J. Chem. Phys.* **2004**, *120*, 6705–6711.
[30] Nara, J.; Higai, S.; Morikawa, Y.; Ohno, T. *Appl. Surf. Sci.* **2004**, *237*, 433–438.
[31] Pontes, R. B.; Novaes, F. D.; Fazzio, A.; Da Silva, A. J. R. *J. Am. Chem. Soc.* **2006**, *128*, 8996–8997.
[32] Tanibayashi, S.; Tada, T.; Watanabe, S.; Yoshizawa, K. *Jpn. J. Appl. Phys.* **2005**, *44*, 7729–7731.
[33] Heimel, G.; Romaner, L.; Brédas, J.-L.; Zojer, E. *Surf. Sci.* **2006**, *600*, 4548.
[34] Desai, S. K.; Pallassana, V.; Neurock, M. *J. Phys. Chem. B* **2001**, *105*, 9171.
[35] Roudgar, A.; Groß, A. *Chem. Phys. Lett.* **2005**, *409*, 157.
[36] Roudgar, A.; Groß, A. *Surf. Sci.* **2005**, *597*, 42.
[37] Reuter, K.; Scheffler, M. *Phys. Rev. B* **2001**, *65*, 035406.
[38] Kresse, G.; Furthmüller, J. *Phys. Rev. B* **1996**, *54*, 11169.
[39] Perdew, J. P.; Burke, K.; Ernzerhof, M. *Phys. Rev. Lett.* **1996**, *77*, 3865.
[40] Blöchl, P. E. *Phys. Rev. B* **1994**, *50*, 17953.
[41] Kresse, G.; Joubert, D. *Phys. Rev. B* **1999**, *59*, 1758.
[42] Chiang, T.-C. *Surf. Sci. Rep.* **2000**, *39*, 181.
[43] Kiejna, A.; Peisert, J.; Scharoch, P. *Surf. Sci.* **2002**, *432*, 54.
[44] Bilić, A.; Reimers, J. R.; Hush, N. S. *J. Chem. Phys.* **2005**, *122*, 094708.
[45] Gottschalck, J.; Hammer, B. *J. Chem. Phys.* **2002**, *116*, 784–790.
[46] Henkelman, G.; Jónsson, H. *J. Chem. Phys.* **2000**, *113*, 9978.
[47] Michaelides, A. *Appl. Phys. A* **2006**, *85*, 415.
[48] Taylor, C. D.; Wasileski, S. A.; Filhol, J.-S.; Neurock, M. *Phys. Rev. B* **2006**, *73*, 165402.
[49] Kim, Y.-T.; McCarley, R. L.; Bard, A. J. *J. Phys. Chem.* **1992**, *96*, 7416.
[50] Tersoff, J.; Hamann, D. R. *Phys. Rev. Lett.* **1983**, *50*, 1998.
[51] Hong, S.; Kim, H. *J. Korean Phys. Soc.* **2006**, *49*, 2362.
[52] Sinnokrot, M. O.; Sherrill, C. D. *J. Phys. Chem. A* **2004**, *108*, 10200.
[53] Loffreda, D.; Delbecq, F.; Sautet, P. *Chem. Phys. Lett.* **2005**, *405*, 434.
[54] Debye, P.; Hückel, E. *Phys. Z.* **1923**, *24*, 185.